

# SIMULTANEOUS LOW-RANK COMPONENT AND GRAPH ESTIMATION FOR HIGH-DIMENSIONAL GRAPH SIGNALS: APPLICATION TO BRAIN IMAGING

Liu Rui, Hossein Nejati, Seyed Hamid Safavi, Ngai-Man Cheung

Singapore University of Technology and Design (SUTD), Singapore 487372

## ABSTRACT

We propose an algorithm to uncover the intrinsic low-rank component of a high-dimensional, graph-smooth and grossly-corrupted dataset, under the situations that the underlying graph is unknown. Based on a model with a low-rank component plus a sparse perturbation, and an initial graph estimation, our proposed algorithm simultaneously learns the low-rank component and refines the graph. Our evaluations using synthetic and real brain imaging data in unsupervised and supervised classification tasks demonstrate encouraging performance.

**Index Terms**— Graph Signal Processing, Low Rank, Dimensionality Reduction, Graph Learning, Brain Imaging

## 1. INTRODUCTION

We consider the problem of uncovering the intrinsic low rank component of a high-dimensional dataset. We further focus on data that resides on a certain graph and the data changes smoothly between the connected vertices [1]. In many problems, the underlying graph is unknown or inexact [2, 3, 4]. For example, the graph may be estimated from the input data which is grossly corrupted. We propose an algorithm to estimate the low-rank component of the data, using the graph smoothness assumption to assist the estimation. Our algorithm also simultaneously and iteratively refines the graph to improve the effectiveness of the graph smoothness constraint, thereby increasing the quality of low-rank component estimation.

High-dimensional data is common in many engineering areas such as image / video processing, biomedical imaging, computer networks and transportation networks. We are specifically interested in automatic analysis of brain imaging data. In many cases, the task is to find the spatiotemporal neural signature of a task, by performing classification on cortical activations evoked by different stimuli [5, 6]. Common brain imaging techniques are Electroencephalography (EEG) and Magnetoencephalography (MEG). These measurements are high-dimensional spatiotemporal data. For instance, in our experiments, we use a recumbent Elekta MEG scanner with 306 sensors to record the brain activity for 1100 milliseconds. Furthermore, the measurements are degraded by various types of noise (e.g., sensor noise, ambient magnetic field noise, etc.) and the noise model is complicated (potentially non-Gaussian). The high-dimensionality and noise limit both the speed and accuracy of the signal analysis, that may result in unreliable signature modeling for classification. The high-dimensionality of these signals also increases the complexity of the classifier.

Note that it has been recognized that there are patterns of anatomical links, or statistical dependencies or causal interactions between distinct units within a nervous system [7]. Some techniques have also been developed to estimate this *brain connectivity graph* [8, 9]. However, this task is complicated and in many cases the estimated

graph may not be accurate. Our contribution is to develop a robust algorithm to determine the reduced dimensionality components that include task-related information, under the assumption that the brain imaging data is graph-smooth but the knowledge of the graph is imperfect. Specifically, our contributions are: (i) based on a model with a low-rank component plus a sparse perturbation, and an initial graph estimation, we propose an algorithm to simultaneously learn the low-rank component and the graph; (ii) we derive the learning steps using ADMM [10]; (iii) we evaluate the algorithm using synthetic and real brain imaging data in unsupervised and supervised classification tasks.

## 1.1. Related Work

This work is inspired by [2]. While the focus of [2] is to learn the connectivity graph topology, their algorithm also estimates some noise-free version of the input data as by-product. Gaussian noise model and Frobenius norm optimization are employed in [2]. Therefore, their work is suitable for problem when noise is small. In our work, starting from a model with a low-rank component plus a sparse perturbation, and an initial graph estimation, we adopt the idea of [2] to incrementally refine the underlying connectivity graph, thereby better low-rank estimation of the data can be obtained. As will be shown in our experiment, our method can perform better with high-dimensional graph data *grossly* corrupted by complicated noise, such as brain imaging signals. In addition to [2], learning a graph from smooth signals has attracted a fair amount of interests recently [3, 4]. These works focus on learning the graph, and advanced formulations (e.g., matrix optimization problem) have been derived. Estimation of the brain connectivity graph using a Gaussian noise model has been proposed in [11]. On the other hand, focusing on low-rank estimation, some works have proposed to incorporate spectral graph regularization [12, 13, 14]. Their graphs are *fixed* in their algorithms, pre-computed from the noisy input data. On the contrary, our algorithm uses the improved low-rank estimation to refine the graph, which in turn is used to improve the quality of the low-rank estimation. Besides, graph signal processing has been applied to a few different brain imaging tasks. In [15], graph Fourier transform is applied to decompose brain signals into low, medium, and high frequency components for analysis of functional brain networks properties. [16] uses the eigenvectors of the graph Laplacian to approximate the intrinsic subspace of high-dimensional brain imaging data. They experimented different brain connectivity estimations to compute the graph. Graph signal processing has also been shown to be useful in image compression [17], temperature data [2], wireless sensor data [18]. A few signal features motivated by graph signal processing have also been proposed [19, 20]. Moreover, several linear / nonlinear dimensionality methods have been proposed that make use of the graph Laplacian of the sample affinity graphs [21, 22, 23]. These methods are geometrically motivated, aim to preserve the local

structures of the data, and involve different algorithms compared to our work.

## 2. SIMULTANEOUS LOW RANK AND GRAPH ESTIMATION

We consider  $\mathbf{X} = (\mathbf{x}_1, \dots, \mathbf{x}_n) \in \mathbb{R}^{p \times n}$ , the high dimensional data matrix that consists of  $n$   $p$ -dimensional data points. For our brain imaging data,  $\mathbf{X}$  are the measurements by the  $p$  sensors at the  $n$  time instants, i.e.,  $p$  time series. We assume the data points have low intrinsic dimensionality and lie near some low-dimensional subspace. We assume the following mathematical model for the data:

$$\mathbf{X} = \mathbf{L}_0 + \mathbf{M}_0 \quad (1)$$

$\mathbf{L}_0 \in \mathbb{R}^{p \times n}$  is the low-rank component of the data matrix that is of primary interest in this paper, and  $\mathbf{M}_0 \in \mathbb{R}^{p \times n}$  is a perturbation matrix. We assume that  $\mathbf{M}_0$  can have arbitrarily large magnitude but its support is sparse.

Principal component analysis (PCA) is the most popular technique for determining the low-rank component with application domains ranging from image, video, signal, web content, to network. The *classical PCA* finds the projection  $\mathbf{Q}^T \in \mathbb{R}^{k \times n}$  of  $\mathbf{X}$  in a  $k$ -dimensional ( $k \leq p$ ) linear space characterized by an orthogonal basis  $\mathbf{V} \in \mathbb{R}^{p \times k}$ , by solving the following optimization:

$$\begin{aligned} & \underset{\mathbf{V}, \mathbf{Q}}{\text{minimize}} \quad \|\mathbf{X} - \mathbf{V}\mathbf{Q}^T\|_F^2 \\ & \text{subject to} \quad \mathbf{V}^T \mathbf{V} = \mathbf{I} \end{aligned} \quad (2)$$

The  $\mathbf{V}$  and  $\mathbf{Q}^T$  matrices are known as principal components and projected data points, respectively.  $\mathbf{L} = \mathbf{V}\mathbf{Q}^T \in \mathbb{R}^{p \times n}$  is the approximation of the low-rank component. The classical PCA suffers from a few disadvantages. First, it is susceptible to grossly corrupted data in  $\mathbf{X}$ . Second, it does not consider the implicit data manifold information.

Candes *et al.* [24] addressed the first issue by designing *Robust PCA*, which is robust to outliers by directly recovering the low-rank matrix  $\mathbf{L}$  from the grossly corrupted  $\mathbf{X}$ :

$$\begin{aligned} & \underset{\mathbf{L}, \mathbf{M}}{\text{minimize}} \quad \|\mathbf{L}\|_* + \delta \|\mathbf{M}\|_1 \\ & \text{subject to} \quad \mathbf{X} = \mathbf{L} + \mathbf{M} \end{aligned} \quad (3)$$

$\|\cdot\|_*$  denotes the nuclear norm which is used as a convex surrogate of rank.

In this work we propose to extend (3) with an additional graph smoothness regularization, while the underlying graph topology that captures the data correlation could be *unknown* or *inexact* (thus some refinement is needed):

$$\begin{aligned} & \underset{\mathbf{L}, \mathbf{M}, \Phi_f}{\text{minimize}} \quad \|\mathbf{L}\|_* + \delta \|\mathbf{M}\|_1 + \gamma \text{tr}(\mathbf{L}^T \Phi_f \mathbf{L}) + \beta \|\Phi_f\|_F^2 \\ & \text{subject to} \quad \mathbf{X} = \mathbf{L} + \mathbf{M}, \\ & \quad \Phi_f \in \mathcal{L} \end{aligned} \quad (4)$$

Here  $\Phi_f$  is the graph Laplacian of the feature graph  $\mathcal{G}$  describing the correlation between individual features:  $\mathcal{G} = (\mathcal{V}, \mathcal{E}, \mathbf{W})$  consists of a finite set of vertices  $\mathcal{V}$ , with  $|\mathcal{V}| = p$ , a set of edges  $\mathcal{E}$ , and a weighted adjacency matrix  $\mathbf{W} = \{W_{i,j} | W_{i,j} \geq 0\}$ , with  $W_{i,j}$  quantifying the similarity between the  $i$ -th and  $j$ -th features of the  $p$ -dimensional measurement vectors.  $\Phi_f = \mathbf{D} - \mathbf{W}$ , with  $\mathbf{D}$  being the diagonal degree matrix.  $\mathcal{L}$  is the set of all valid  $p \times p$  graph Laplacian  $\Phi$ :

$$\mathcal{L} = \{\Phi : \Phi_{ij} = \Phi_{ji} \leq 0, \Phi_{ii} = -\sum_{j \neq i} \Phi_{ij}\} \quad (5)$$

As will be further discussed in Section 3, we solve (4) iteratively using alternating minimization with the following justifications:

- **$\mathbf{L}, \mathbf{M}$  given  $\Phi_f$ :** For a given  $\Phi_f$  (even a rough estimate),  $\text{tr}(\mathbf{L}^T \Phi_f \mathbf{L})$  imposes an additional constraint on the underlying (unknown) low-rank data  $\mathbf{L}$ . Specifically,

$$\text{tr}(\mathbf{L}^T \Phi_f \mathbf{L}) = \frac{1}{2} \sum_{i,j} W_{i,j} \|\tilde{l}_i - \tilde{l}_j\|^2, \quad (6)$$

where  $\tilde{l}_i \in \mathbb{R}^n$  is the  $i$ -th row vector of  $\mathbf{L}$ . Therefore,  $\text{tr}(\mathbf{L}^T \Phi_f \mathbf{L})$  in (4) forces the row  $i$  and  $j$  of  $\mathbf{L}$  to have similar values if  $W_{i,j}$  is large. Note that in our brain imaging data, individual rows represent the time series captured by sensors. Thus,  $\text{tr}(\mathbf{L}^T \Phi_f \mathbf{L})$  forces the low-rank representations of the time series to be similar for highly correlated sensors. Prior information regarding measurement correlation (such as the physical distance between the capturing sensors) can be incorporated as the initial  $\Phi_f$  to bootstrap the estimation of  $\mathbf{L}$ .

- **$\Phi_f$  given  $\mathbf{L}, \mathbf{M}$ :** On the other hand, for a given estimate of the low-rank data  $\mathbf{L}$ ,  $\text{tr}(\mathbf{L}^T \Phi_f \mathbf{L})$  guides the refinement of  $\Phi_f$  and hence the underlying connectivity graph  $\mathcal{G}$ . In particular, a graph  $\mathcal{G}$  that is consistent with the signal variation in  $\mathbf{L}$  is favored: large  $W_{i,j}$  if row  $i$  and  $j$  of  $\mathbf{L}$  have similar values. In many problems, the given graph for a problem can be noisy (e.g., the graph is estimated from the noisy data itself [13, 14]). The proposed formulation iteratively improves  $\Phi_f$  using the refined low-rank data. The improved  $\Phi_f$  in turn facilitates the low-rank data estimation.

## 3. LEARNING ALGORITHM

We propose to solve the problem in Eq (4) with alternating minimization scheme where, at each step, we fix one or two variables and update the other variable.

At the first step, for a given  $\Phi_f$ , we solve the following optimization problem using ADMM[10] with respect to  $\mathbf{L}$  and  $\mathbf{M}$ :

$$\begin{aligned} & \underset{\mathbf{L}, \mathbf{M}}{\text{minimize}} \quad \|\mathbf{L}\|_* + \delta \|\mathbf{M}\|_1 + \gamma \text{tr}(\mathbf{L}^T \Phi_f \mathbf{L}) \\ & \text{subject to} \quad \mathbf{X} = \mathbf{L} + \mathbf{M}, \end{aligned} \quad (7)$$

At the second step,  $\mathbf{L}$  and  $\mathbf{M}$  are fixed and we solve the following optimization problem with respect to  $\Phi_f$ :

$$\begin{aligned} & \underset{\Phi_f}{\text{minimize}} \quad \gamma \text{tr}(\mathbf{L}^T \Phi_f \mathbf{L}) + \beta \|\Phi_f\|_F^2 \\ & \text{subject to} \quad \Phi_f \in \mathcal{L} \end{aligned} \quad (8)$$

For equation (8), we also apply ADMM on it. It can be written as:

$$\begin{aligned} & \underset{\Phi_f}{\text{minimize}} \quad \gamma \text{tr}(\mathbf{L}^T \Phi_f \mathbf{L}) + \beta \|\Phi_f\|_F^2 + \frac{\rho}{2} \|z - \Phi_f\|_F^2 \\ & \text{subject to} \quad \Phi_f - z = 0, \\ & \quad \Phi_f \in \mathcal{L} \end{aligned} \quad (9)$$

We can form the augmented Lagrangian:

$$\begin{aligned} L_\rho(\Phi_f, z, u) = & \gamma \text{tr}(\mathbf{L}^T \Phi_f \mathbf{L}) + \beta \|\Phi_f\|_F^2 \\ & + \frac{\rho}{2} \|z - \Phi_f\|_F^2 + \langle u, z - \Phi_f \rangle \end{aligned} \quad (10)$$

Then we can get the following formula to update for  $\Phi_f$ ,  $z$  and  $u$ :

Methods	Low Rank Matrix	Graph Matrix
Proposed Method	<b>1.024</b>	<b>0.2605</b>
GL-SigRep	6.0395	0.4884
RPCA	11.1462	-
RPCAG	2.5693	-

**Table 1:** Comparison of low rank matrix error and estimated graph error for synthetic data.

$$\begin{aligned}
\Phi_f^{k+1} &:= \frac{\rho z^k - \gamma \mathbf{L}^T \mathbf{L} + u}{\frac{\beta}{2} + \rho} \\
z^{k+1} &:= \prod_{\mathcal{L}} (\Phi_f^{k+1} - \frac{1}{\rho} u^k) \\
u^{k+1} &:= u^k + \frac{1}{k} (z^{k+1} - \Phi_f^{k+1})
\end{aligned} \tag{11}$$

where  $\rho > 0$  is the Lagrangian parameter and  $\prod_{\mathcal{L}}$  is the Euclidean projection onto set  $\mathcal{L}$ .

## 4. EXPERIMENT

### 4.1. Synthetic Experiment

In this synthetic experiment, we generate low-rank, graph-smooth and grossly-corrupted data. We generate synthetic data with the following model:

$$X_{noisy} = L_0 + M_0 \tag{12}$$

where  $L_0$  is a low rank matrix with rank  $r$  and  $M_0$  is the sparse matrix.

We generate  $L_0 \in \mathbb{R}^{p \times n}$  as a product  $L_0 = XY^T$  where  $X \in \mathbb{R}^{p \times r}$  and  $Y \in \mathbb{R}^{n \times r}$ .  $L_0$  is also graph-smooth and generated as follows. The (ground-truth) graph consists of  $p$  nodes, with each pair of nodes having a probability of  $q$  to be connected together. The edge weights between different nodes are drew uniformly from 0 to 1 and presented in a  $p \times p$  symmetric adjacency matrix  $W$ . We calculate the Laplacian matrix  $A$  from  $W$ , compute the eigenvectors and eigenvalues of  $A$ . The eigenvectors, corresponding to top  $r$  eigenvalues, are selected to be the columns of  $X$ . For matrix  $Y$ , the entries are independently sampled from a  $N(0, 1/p)$  distribution. Therefore,  $L_0$  is low-rank and graph-smooth. We introduce  $k = \|M_0\|_0/p^2 = 10\%$  errors in the matrix  $M_0$  from an i.i.d Bernoulli distribution. Each corrupted entry takes a value  $\pm 1$  with a probability  $k/2$ .

We compare the proposed method, RPCA[24], RPCAG[13] and GL-SigRep[25] on the data to estimate the low rank matrix and the graph matrix. The estimation accuracies are evaluated by the reconstruction errors:  $\|\hat{L} - L_0\|_F / \|L_0\|_F$  and  $\|\hat{\Phi}_f - A\|_F / \|A\|_F$ . Table 1 shows the results on synthetic data generated by the Eq (12) with  $p = 40, n = 200, r = 4, k = 10\%, q = 0.3$ . All the methods are initialized with the *same* feature similarity graph computed using the procedure in [14]. In particular, the graph is constructed between the features of the data matrix (the rows of  $X_{noisy}$ ) with a K-nearest neighbor strategy ( $K = 10$ ). We consider each row as a node, then we search for the  $K$  closest neighbors for every node using the Euclidean distance and connect them. Then we generate the weights for connected nodes with a Gaussian kernel function, and compute the adjacency matrix.

As shown in Table 1, the low rank approximation of proposed method achieves the smallest error. For the estimate graph matrix,

the proposed method also achieves the smallest estimation error. Synthetic experiment results show that the proposed method can achieve good performance on extracting low rank approximation and the underlying graph from non-Gaussian noisy data.

### 4.2. Brain Imaging Data Experiment

We apply the proposed method on a high-dimensional brain imaging dataset, in order to extract the brain connectivity graph and the low rank approximation from the high dimensionality. This is practically useful: due to the high dimensionality, low signal-to-noise ratio, and few number of samples, it is challenging to estimate the low rank approximation in these studies. The brain imaging dataset used here is magnetoencephalography (MEG) signal recordings of brain activities in response to two categories of visual stimuli: faces and objects. MEG signals from 306 sensors have been recorded as 16 subjects were randomly exposed to 320 face images and 192 non-face images. The (unsupervised and supervised) classification tasks in this experiment are to distinguish between signals evoked by face images and signals evoked by non-face images.

#### 4.2.1. Initial graph matrix

In the proposed method, a suitable starting point is important for solving the optimization problem. We therefore initialize  $\Phi_f$  with the brain connectivity matrix generated with the resting state measurements (signals from 100ms before the stimuli presentation). Note that our method and all other methods are initialized with the same connectivity matrix. Three different types of brain connectivity graphs are commonly used in the literature: structural connectivity, functional connectivity and effective connectivity. In this paper we use a correlation connectivity, a basic functional connectivity capturing the statistical dependencies between different regions [16]. Given the resting state sensor measurements at two spatially-separated brain regions:  $X$  and  $Y$ , written as  $x_t$  and  $y_t$  for times  $t = 1, 2, \dots, T$ , the edge weight for correlation connectivity between  $X$  and  $Y$  can be computed as:

$$\begin{aligned}
w_{X,Y} &= \frac{\sum_{t=1}^T (x_t - \bar{x})(y_t - \bar{y})}{(T-1)s_x s_y} \\
&= \frac{\sum_{t=1}^T (x_t - \bar{x})(y_t - \bar{y})}{\sqrt{\sum_{t=1}^T (x_t - \bar{x})^2 \sum_{t=1}^T (y_t - \bar{y})^2}}
\end{aligned} \tag{13}$$

where  $\bar{x}$  and  $\bar{y}$  are the sample mean of  $X$  and  $Y$ .  $s_x$  and  $s_y$  are sample standard deviation of  $X$  and  $Y$ . We use the absolute value of each edge weight in correlation connectivity matrix as the entry in the adjacency matrix  $W$ . Then, the Laplacian matrix  $A = D - W$  is used as the initialization.

#### 4.2.2. Brain Imaging Data Experiment Results

To evaluate the performance of proposed method, we use both an unsupervised classifier, K-means, and a supervised classifier, SVM. The task is to classify the outputs into face and non-face classes. We compare these methods based on their classification accuracy as well as compatibility of their connectivity graph matrix to the related neuroscience findings on suggested cortical regions involving face processing.

In this experiment, we choose the data from two time slots, namely 96ms to 105ms and 141ms to 150ms after the stimuli presentation. These time slots are reported as the initial visual stimuli processing time point, and face processing time point (also known

Methods	K-means	SVM
Proposed Method	<b>58.19%</b>	<b>73.67%</b>
GL-SigRep	52.30%	65.99%
RPCA	52.66%	66.31%
RPCAG	52.03%	71.85%

**Table 2:** Classification performance (accuracies) for brain imaging data(Time: 96ms-105ms)

Methods	K-means	SVM
Proposed Method	<b>55.68%</b>	69.43%
GL-SigRep	51.66%	68.22%
RPCA	51.41%	68.45%
RPCAG	50.60%	<b>71.91%</b>

**Table 3:** Classification performance (accuracies) for brain imaging data(Time: 141-150ms)

as N170 marker) in the related neuroscience literature (e.g. see [26, 27, 28, 29]).

Our proposed method, GL-SigRep, RPCA and RPCAG output some low rank estimation  $L$ . We decompose the low rank matrix  $L$  using SVD, select the components attributed to 90% of data energy, project the data onto these components to obtain low-dimensionality representations, and perform classification on the reduced dimension data.

Table 2 and 3 show the classification results for different methods on the two time slots assessed. For unsupervised classification, the proposed method gives the best results for both time slots. For supervised classification, the proposed method outperforms other methods during 96ms to 105ms. For 141ms to 150ms, though the performance of the proposed method is not as high as RPCAG.

For another comparison, in Figure 1 we visualize the estimated graph matrix  $\Phi_f$  by our method as well as the GL-SigRep method, by projecting the graph connectivity weights on the MEG sensor locations. Comparing these graph visualizations at around 100ms (see Figure 1-a & b), we can see that GL-SigRep focuses on the frontal cortical regions, while our method tends to span from frontal to occipital regions. It is well known that the frontal cortex does not process the visual information at this time, and the information is still being processed at early visual cortex at occipital regions (e.g. see [27, 29]). Therefore the connectivity graph including the occipital region may indicate more successful estimation of graph connectivity by our method.

The connectivity graph estimated during 141ms to 150ms(see Figure 1-c & d) is particularly interesting. While the graph from GL-SigRep remains focused on the frontal cortical regions, our method selects regions from far right from the cortex that spans from the occipital regions up to the right frontal regions. This graph connectivity is comparable to the neuroscience findings on face perception, and specifically the N170 marker. In several studies such as [26, 28], the early visual cortex (at the occipital region) and the fusiform gyrus (at the occipitotemporal region) are suggested for processing face perception during about 141ms to 150ms after presentation of face stimuli, also known as N170 marker (named after its appearance at 170ms in EEG studies). In this work, our technique reveals almost the same regions as *important* graph components for face perception. This compatibility with neuroscience literature further supports our proposed method over others.

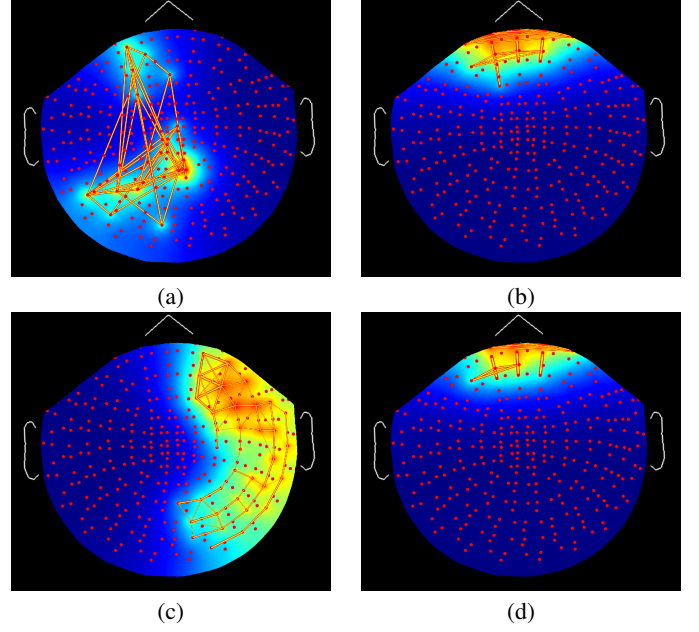


**Fig. 1:** Graph Estimation results. (a) and (b) are the results for the propose method and GL-SigRep, respectively, on signal data from 96ms - 105ms; (c) and (d) are the results for the proposed method and GL-SigRep, respectively, on signal data from 141ms - 150ms

## 5. CONCLUSION

We propose an algorithm in learning the low rank component and graph simultaneously. It is suitable for cases where the perturbations on the low rank components are grossly but sparse. We showed that the our proposed method on both synthetic data and brain imaging data is competitive. Our method achieves good performance on both low rank approximation and graph estimation. In addition, when applying to the brain imaging data, our method could recover a connectivity graph that is more compatible to the neuroscience literature, indicating its better estimation of the true underlying graph.

## 6. REFERENCES

- [1] David Shuman, Sunil K Narang, Pascal Frossard, Antonio Ortega, Pierre Vandergheynst, et al., “The emerging field of signal processing on graphs: Extending high-dimensional data analysis to networks and other irregular domains,” *Signal Processing Magazine, IEEE*, vol. 30, no. 3, pp. 83–98, 2013.
- [2] Xiaowen Dong, Dorina Thanou, Pascal Frossard, and Pierre Vandergheynst, “Laplacian matrix learning for smooth graph signal representation,” in *Proc. ICASSP*, 2015.
- [3] Eduardo Pavez and Antonio Ortega, “Generalized laplacian precision matrix estimation for graph signal processing,” in *Proc. ICASSP*, 2016.
- [4] Vassilis Kalofolias, “How to learn a graph from smooth signals,” in *AISTATS 2016*, 2016.
- [5] Kleovoulos Tsourides, Shahriar Shariat, Hossein Nejati, Tapan K Gandhi, Annie Cardinaux, Christopher T Simons, Ngai-Man Cheung, Vladimir Pavlovic, and Pawan Sinha, “Neural correlates of the food/non-food visual distinction,” *Biological Psychology*, 2016.
- [6] H. Nejati, K. Tsourides, V. Pomponiu, E.C. Ehrenberg, Ngai-Man Cheung, and P. Sinha, “Towards perception awareness: Perceptual event detection for brain computer interfaces,” in *EMBC2015*, Aug 2015, pp. 1480–1483.
- [7] Ed Bullmore and Olaf Sporns, “Complex brain networks: graph theoretical analysis of structural and functional systems,” *Nature Reviews Neuroscience*, vol. 10, no. 3, pp. 186–198, 2009.
- [8] James S Hyde and Andrzej Jesmanowicz, “Cross-correlation: an fmri signal-processing strategy,” *NeuroImage*, vol. 62, no. 2, pp. 848–851, 2012.
- [9] Andrea Brovelli, Mingzhou Ding, Anders Ledberg, Yonghong Chen, Richard Nakamura, and Steven L Bressler, “Beta oscillations in a large-scale sensorimotor cortical network: directional influences revealed by granger causality,” *Proceedings of the National Academy of Sciences of the United States of America*, vol. 101, no. 26, pp. 9849–9854, 2004.
- [10] Stephen Boyd, Neal Parikh, Eric Chu, Borja Peleato, and Jonathan Eckstein, “Distributed optimization and statistical learning via the alternating direction method of multipliers,” *Foundations and Trends in Machine Learning*, vol. 3, no. 1, pp. 1–122, 2011.
- [11] Chenhui Hu, Lin Cheng, Jorge Sepulcre, Georges El Fakhri, Yue M. Lu, and Quanzheng Li, “A graph theoretical regression model for brain connectivity learning of alzheimer’s disease,” in *ISBI2013*, San Francisco, CA, 7–11 Apr. 2013.
- [12] Bo Jiang, Chris Ding, Bin Luo, and Jin Tang, “Graph-Laplacian PCA: Closed-form solution and robustness,” in *CVPR*, 2013, pp. 3490–3496.
- [13] Nauman Shahid, Vassilis Kalofolias, Xavier Bresson, Michael Bronstein, and Pierre Vandergheynst, “Robust principal component analysis on graphs,” in *Proceedings of International Conference on Computer Vision*, Santiago, Chile, 2015, pp. 2812–2820.
- [14] Nauman Shahid, Nathanael Perraudin, Vassilis Kalofolias, Gilles Puy, and Pierre Vandergheynst, “Fast robust PCA on graphs,” *arXiv:1507.08173v2 [cs.CV] 25 Jan 2016*, pp. 1–17, 2016.
- [15] Weiyu Huang, Leah Goldsberry, Nicholas F Wymbs, Scott T Grafton, Danielle S Bassett, and Alejandro Ribeiro, “Graph frequency analysis of brain signals,” *arXiv preprint arXiv:1512.00037v2*, 2016.
- [16] Liu Rui, Hossein Nejati, and Ngai-Man Cheung, “Dimensionality reduction of brain imaging data using graph signal processing,” in *ICIP. IEEE*, 2016, pp. 1329–1333.
- [17] Wei Hu, Gene Cheung, Antonio Ortega, and Oscar C Au, “Multiresolution graph fourier transform for compression of piecewise smooth images,” *Image Processing, IEEE Transactions on*, vol. 24, no. 1, pp. 419–433, 2015.
- [18] Hilmi E Egilmez and Antonio Ortega, “Spectral anomaly detection using graph-based filtering for wireless sensor networks,” in *ICASSP. IEEE*, 2014, pp. 1085–1089.
- [19] Xiaowen Dong, Antonio Ortega, Pascal Frossard, and Pierre Vandergheynst, “Inference of mobility patterns via spectral graph wavelets,” in *ICASSP. IEEE*, 2013, pp. 3118–3122.
- [20] Jieqi Kang, Shan Lu, Weibo Gong, and Patrick A Kelly, “A complex network based feature extraction for image retrieval,” in *ICIP. IEEE*, 2014, pp. 2051–2055.
- [21] M. Belkin and P. Niyogi, “Laplacian eigenmaps for dimensionality reduction and data representation,” *Neural Computation*, vol. 15, no. 6, pp. 1373–1396, 2003.
- [22] Xiaofei He and Partha Niyogi, “Locality preserving projection,” in *Proceedings of NIPS*, 2003.
- [23] Shuicheng Yan, Dong Xu, Benyu Zhang, and Stephen Lin, “Graph embedding and extensions: a general framework for dimensionality reduction,” *IEEE Transactions on Pattern Analysis and Machine Intelligence*, 2007.
- [24] Emmanuel J. Candès, Xiaodong Li, Yi Ma, and John Wright, “Robust principal component analysis?,” *Journal of the ACM*, vol. 58, no. 3, pp. 11:1–11:37, May 2011.
- [25] Xiaowen Dong, Dorina Thanou, Pascal Frossard, and Pierre Vandergheynst, “Learning laplacian matrix in smooth graph signal representations,” *arXiv preprint arXiv:1406.7842v3*, 2014.
- [26] David I. Perrett, Amanda J. Mistlin, and Andrew J. Chitty, “Visual neurones responsive to faces,” *Trends in Neurosciences*, vol. 10, no. 9, pp. 358 – 364, 1987.
- [27] S. Thorpe, D. Fize, and C. Marlot, “Speed of processing in the human visual system,” *Nature*, vol. 381, no. 6582, pp. 520–2, 1996.
- [28] Jia Liu, Alison Harris, and Nancy Kanwisher, “Stages of processing in face perception: an MEG study,” *Nature neuroscience*, vol. 5, no. 9, pp. 910–916, Sept. 2002.
- [29] R. Desimone, “Face-selective cells in the temporal cortex of monkeys,” *Journal of Cognitive Neuroscience*, vol. 3, no. 1, pp. 1–8, Jan. 2006.